

## THE SIGNATURE OF $^{44}\text{Ti}$ IN CASSIOPEIA A REVEALED BY IBIS/ISGRI ON *INTEGRAL*

M. RENAUD,<sup>1,2</sup> J. VINK,<sup>3</sup> A. DECOURCHELLE,<sup>1,4</sup> F. LEBRUN,<sup>1,2</sup> P. R. DEN HARTOG,<sup>5</sup> R. TERRIER,<sup>2</sup> C. COUVREUR,<sup>1</sup>  
J. KNÖDLSEDER,<sup>6</sup> P. MARTIN,<sup>6</sup> N. PRANTZOS,<sup>7</sup> A. M. BYKOV,<sup>8</sup> AND H. BLOEMEN<sup>5</sup>

Received 2006 May 10; accepted 2006 June 29; published 2006 August 1

### ABSTRACT

We report the detection of both the 67.9 and 78.4 keV  $^{44}\text{Sc}$   $\gamma$ -ray lines in Cassiopeia A with the *INTEGRAL* IBIS/ISGRI instrument. Besides the robustness provided by spectroimaging observations, the main improvements compared to previous measurements are a clear separation of the two  $^{44}\text{Sc}$  lines together with an improved significance of the detection of the hard X-ray continuum up to 100 keV. These allow us to refine the determination of the  $^{44}\text{Ti}$  yield and to constrain the nature of the nonthermal continuum emission. By combining COMPTEL, *BepoSAX* PDS and ISGRI measurements, we find a line flux of  $(2.5 \pm 0.3) \times 10^{-5} \text{ cm}^{-2} \text{ s}^{-1}$  leading to a synthesized  $^{44}\text{Ti}$  mass of  $1.6_{-0.3}^{+0.6} \times 10^{-4} M_{\odot}$ . This high value suggests that Cas A is peculiar in comparison to other young supernova remnants, from which so far no line emission from  $^{44}\text{Ti}$  decay has been unambiguously detected.

*Subject headings:* gamma rays: observations — ISM: individual (Cassiopeia A) — nuclear reactions, nucleosynthesis, abundances — supernova remnants

*Online material:* color figures

### 1. INTRODUCTION

Cassiopeia A (Cas A) is the youngest known supernova remnant (SNR) in the Milky Way, located at a distance of  $3.4_{-0.1}^{+0.3}$  kpc (Reed et al. 1995). The estimate of the supernova is AD  $1671.3 \pm 0.9$ , based on the proper motion of several ejecta knots (Thorstensen et al. 2001). However, an event observed by Flamsteed (AD 1680) could be at the origin of the Cas A remnant (Ashworth 1980; Stephenson & Green 2002). The large collection of data from observations in the radio, infrared, optical, X-ray (see, e.g., Hwang et al. 2004), and up to TeV  $\gamma$ -rays (Aharonian et al. 2001) allows us to study its morphology, composition, cosmic-ray acceleration efficiency, and secular evolution in detail. Young SNRs are thought to be efficient particle accelerators and represent the main galactic production sites of heavy nuclei, some of them being radioactive. Soft  $\gamma$ -ray observations, beyond the thermal X-ray emission ( $\geq 10$  keV), can therefore provide invaluable information in both of these areas by studying the nonthermal continuum and the  $\gamma$ -ray line emission. Cas A then appears to be the best case for such investigations.

Few radioactive isotopes are accessible to  $\gamma$ -ray astronomy for probing cosmic nucleosynthesis (Diehl & Timmes 1998). Among them,  $^{44}\text{Ti}$  is a key isotope for the investigation of the inner regions of core-collapse SNe and their young remnants. This nucleus is thought to be exclusively created in SNe but with a large variation of yields depending on their type. Recent accurate measurements by several independent groups give a

weighted-average  $^{44}\text{Ti}$  lifetime of  $86.0 \pm 0.5$  yr (Ahmad et al. 1998; Görres et al. 1998; Norman et al. 1998; Wietfeldt et al. 1999; Hashimoto et al. 2001). The discovery of the 1157 keV  $^{44}\text{Ca}$   $\gamma$ -ray line emission from the decay chain of  $^{44}\text{Ti}$  ( $^{44}\text{Ti} \rightarrow ^{44}\text{Sc} \rightarrow ^{44}\text{Ca}$ ) with the *Compton Gamma Ray Observatory* (CGRO) COMPTEL (Iyudin et al. 1994) was the first direct proof that this short-lived isotope is indeed produced in SNe. This has been strengthened by the *BepoSAX* Phoswich Detector System (PDS) detection of the two blended low-energy  $^{44}\text{Sc}$  lines at 67.9 and 78.4 keV (Vink et al. 2001). By combining both observations, Vink et al. (2001) deduced a  $^{44}\text{Ti}$  yield of  $(1.5 \pm 1.0) \times 10^{-4} M_{\odot}$ .

This high value compared to those predicted by “standard” models (e.g., Woosley & Weaver 1995, hereafter WW95; Thielemann et al. 1996, hereafter TNH96) as well as improved ones (Rauscher et al. 2002; Limongi & Chieffi 2003) could be due to several effects. First of all, the explosion of Cas A seems to have been intrinsically asymmetric since such asymmetries have recently been observed in the ejecta (Vink 2004; Hwang et al. 2004), and there are indications that its explosion energy was  $\sim 2 \times 10^{51}$  ergs (Laming & Hwang 2003), higher than the canonical value of  $10^{51}$  ergs. The sensitivity of the  $^{44}\text{Ti}$  production to the explosion energy and asymmetries may explain the high  $^{44}\text{Ti}$  yield compared to explosion models (Nagataki et al. 1998).

It is generally accepted that Cas A was formed by the explosion of a massive progenitor, from a  $16 M_{\odot}$  single star (Chevalier & Oishi 2003) to a Wolf-Rayet (W-R) remnant of a very massive ( $< 60 M_{\odot}$ ) precursor (Fesen & Becker 1991). Type Ib explosions, originating from progenitors that have experienced strong mass loss (see Vink 2004, 2005), should on average produce more  $^{44}\text{Ti}$  due to the lower fallback of material on the compact stellar remnant (Woosley et al. 1995). However, there is some debate on the detailed stellar evolution scenario that may have accounted for the low mass of the star prior to the explosion. The amount of oxygen present ( $1-2 M_{\odot}$ ; Vink et al. 1996) suggests a main-sequence mass of  $20 M_{\odot}$ . This may be too low to form a Type Ib progenitor by mass loss in a W-R phase. Moreover, the high surrounding density is better explained if the shock wave is moving through the dense wind of a red supergiant rather than

<sup>1</sup> Service d’Astrophysique, DAPNIA/DSM/CEA, 91191 Gif-sur-Yvette, France; mrenaud@cea.fr.

<sup>2</sup> APC-UMR 7164, 11 Place M. Berthelot, 75231 Paris, France.

<sup>3</sup> Astronomical Institute, Utrecht University, P.O. Box 80000, 3508 TA Utrecht, Netherlands.

<sup>4</sup> AIM-UMR 7158, 91191 Gif-sur-Yvette, France.

<sup>5</sup> SRON Netherlands Institute for Space Research, Sorbonnelaan 2, 3584 AC Utrecht, Netherlands.

<sup>6</sup> Centre d’Etude Spatiale des Rayonnements and Université Paul Sabatier, 31028 Toulouse, France.

<sup>7</sup> Institut d’Astrophysique de Paris, 75014 Paris, France.

<sup>8</sup> A.F. Ioffe Institute for Physics and Technology, 194021 St. Petersburg, Russia.

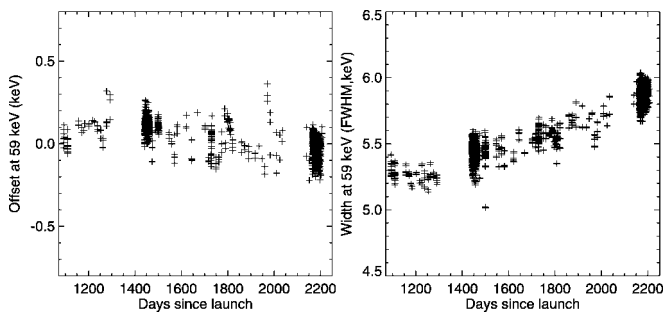


FIG. 1.—Position (*left*) and width (*right*) of the W K $\alpha$  background line.

the more tenuous wind of a W-R. Therefore, it has been recently suggested that the low mass of the progenitor is the result of a common envelope evolutionary phase in a binary system (Young et al. 2006). The authors demonstrated that such a scenario of a 15–25  $M_{\odot}$  progenitor that lost its hydrogen envelope due to a binary interaction can match the main observational constraints. In any case, the  $^{44}\text{Ti}$  production is highly sensitive to details of the explosion as well as nuclear reaction rates. It is of interest to point out that the major  $^{44}\text{Ti}$  production reaction  $^{40}\text{Ca}(\alpha, \gamma)^{44}\text{Ti}$  has been revised (Nassar et al. 2006), implying an increase of the  $^{44}\text{Ti}$  production by a factor of  $\sim 2$ .

In addition to the  $^{44}\text{Sc}$   $\gamma$ -ray lines, the hard X-ray spectrum is also of interest for its nonthermal continuum emission and because this underlying continuum is critical to properly measure the  $^{44}\text{Sc}$  line flux. Nevertheless, its nature is still under debate. The nonthermal hard X-ray continuum could be due to either synchrotron radiation of TeV electrons (Allen et al. 1997) or nonthermal bremsstrahlung from suprathermal electrons that have been accelerated by internal shocks (Laming 2001a, 2001b; Vink & Laming 2003). Both cases predict a gradual steepening at high energies, and then reliable continuum flux measurements beyond the two low-energy  $^{44}\text{Sc}$  lines ( $>80$  keV) are necessary, as initiated with the *CGRO* Oriented Scintillation Spectrometer Experiment (OSSE; The et al. 1996). Soft  $\gamma$ -ray observations are therefore critical to better understand the nucleosynthesis and the particle acceleration processes in young SNRs such as Cas A. The Imager on Board the *INTEGRAL* Satellite (IBIS; Ubertini et al. 2003), one of the two main coded mask aperture instruments on board the *International Gamma-Ray Astrophysics Laboratory* (*INTEGRAL*) satellite (Winkler et al. 2003), is best suited to study both the hard X-ray continuum and the line emission thanks to its low-energy (15 keV–1 MeV) camera, the *INTEGRAL* Soft Gamma-Ray Imager (ISGRI; Lebrun et al. 2003). IBIS/ISGRI provides spectroimaging (13' FWHM, 6 keV FWHM at 70 keV) over a large field of view (400 deg $^2$ ) in the energy range 15 keV–1 MeV with a millicrab sensitivity at 70 keV (3  $\sigma$ ,  $\Delta E/E = 2, 10^6$  s). The large field of view allows for long exposures devoted to the simultaneous observation of several sources. In this Letter, we report the results of the spectroimaging analysis of Cas A based on IBIS/ISGRI observations.

## 2. INTEGRAL IBIS OBSERVATIONS AND DATA ANALYSIS

Since its launch, *INTEGRAL* has performed deep open time observations dedicated to the Cassiopeia region, mainly for measuring and constraining the  $^{44}\text{Ti}$  production in the Cas A and Tycho SNRs. Preliminary results on these two young SNRs are reported in Vink (2005) and Renaud et al. (2006), respectively. Moreover, den Hartog et al. (2006) have presented a comprehensive list of the sources detected by IBIS/ISGRI above 20 keV in this region. We have performed a detailed

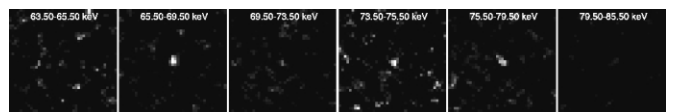


FIG. 2.—IBIS/ISGRI flux images centered on Cas A (2.5°  $\times$  2.5°) in six energy bands. The linear scale is the same for all images, between  $10^{-6}$  and  $4.7 \times 10^{-6} \text{ cm}^{-2} \text{ s}^{-1} \text{ keV}^{-1}$ . Note that the noise in the images depends on the energy bandwidths. [See the electronic edition of the Journal for a color version of this figure.]

analysis of  $\sim 1800$  pointings or science windows (scw's), each of them lasting typically between 1800 and 3500 s during which the telescopes are pointed at a fixed direction. We have selected pointings at less than 11° from Cas A and removed those for which the Veto and ISGRI ( $\geq 500$  keV) count rates were above  $3.5 \times 10^4$  and 45 counts s $^{-1}$ , respectively. The total effective time is then  $\sim 3.2$  Ms (over  $\sim 4.5$  Ms of total exposure time).

For  $\gamma$ -ray line studies, the most critical part of the IBIS/ISGRI data analysis is the energy correction of detected events. The spectral performance of the ISGRI camera depends on the alignment of the pixel gains and offsets. Based on more than 2 years of observations, a fine in-flight calibration has been done by taking into account several parameters such as the temperature, the accumulated proton irradiation, and the time after the detector switch-on. Moreover, because of the charge loss in the cadmium telluride (CdTe) detectors and in their electronics, the ISGRI spectral response above  $\sim 60$  keV depends on the pulse rise time and a second software correction is needed (Lebrun et al. 2003).

To evaluate the efficiency of all these corrections, we measured the position and the width of the W K $\alpha$  fluorescence background line at 59 keV for each scw. As shown in Figure 1, the dispersion of the 59 keV line position over the 3 years of observations is about 0.1 keV. The spectral degradation observed on the right panel of Figure 1 is due to the irradiation of the detector pixels but is still negligible after 3 years in terms of line sensitivity ( $\sim 5\%$ ). The deconvolution of coded mask images (shadowgrams) removes completely the background only if it is flat. Background structures in the shadowgram produce large-scale structures in the deconvolved image. To avoid them, a background map is first subtracted from the shadowgram. Such correcting background maps were produced by summing a large number of high-latitude observations from all directions. In this way, the shadowgrams of the many weak sources are smeared out on the detector. With more than 2 Ms of exposure time, these ensure the best removal of structures in the detector images, mainly around the fluorescence lines located close to the two low-energy  $^{44}\text{Sc}$  astrophysical lines. We then used the Off-Line Scientific Analysis software (Goldwurm et al. 2003, ver. 5.1) in order to obtain sky images, and we have constructed mosaic images in 14 energy bands (see Figs. 2 and 3).

## 3. RESULTS

In order to estimate the source position of the hard X-ray continuum, we also analyzed the 18–25 keV energy band, which has the best signal-to-noise ratio (S/N) for a steep spectrum such as that of Cas A. We have fitted the source with a two-dimensional elliptical Gaussian with the following parameters: the background level, the position and the value of the maximum, the widths on the two axes, and the rotation angle of the ellipse. We did not find any evidence of a source extent (the two widths are close to 14' FWHM). The fitted position of Cas A is R.A. =  $23^{\text{h}}23^{\text{m}}22^{\text{s}}.6$ , decl. =  $+58^{\circ}49'02''.1$

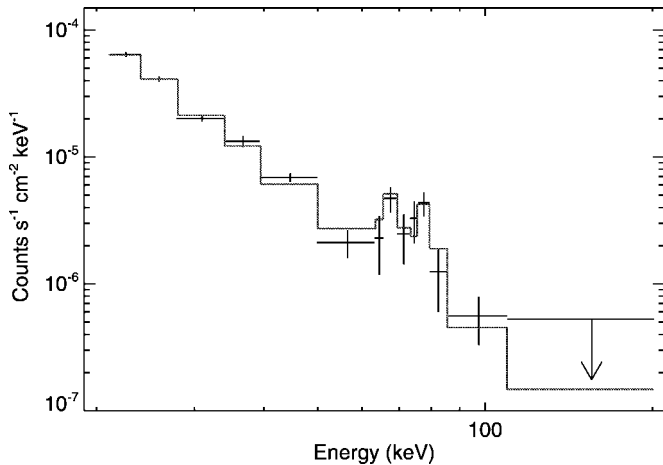


FIG. 3.—IBIS/ISGRI spectrum of Cas A and the best-fit model as described in the text (solid line) with the following boundaries: 21, 24, 28, 34, 39.5, 50, 63.5, 65.5, 69.5, 73.5, 75.5, 79.5, 85.5, 109.5, and 201 keV. The count rates and the model have been divided by the effective ISGRI area at the center of each channel, in order to obtain approximate flux density units. The upper limit above 110 keV is given at the 3  $\sigma$  confidence level. [See the electronic edition of the Journal for a color version of this figure.]

(J2000.0), with a S/N of  $\sim 38$ . According to Gros et al. (2003), the corresponding point-source location error radius at the 90% confidence level is  $\sim 50''$ . Therefore, the full error box is contained within the remnant.

Figure 2 shows IBIS/ISGRI images centered on Cas A in the six energy bands around the two  $^{44}\text{Sc}$  lines, which show that the source brightens at the line energies. For building up the source spectrum, we first measured in each individual sky image the flux and its associated variance at the pixel corresponding to the fitted position in the 18–25 keV energy range. Note that this variance takes into account all uncertainties, in particular those resulting from the background subtraction. We then calculated the weighted mean count rate and corresponding error for each of the 14 energy bands. This spectrum is presented in Figure 3, showing the clear detection of the two low-energy  $^{44}\text{Sc}$  lines. We tested two different models for the continuum emission: the pegged power law `pegpwrlw` in the 21–120 keV band and the `srcut` (Reynolds & Keohane 1999) model in XSPEC version 11.3. This latter is an approximation of the X-ray synchrotron radiation from young SNRs. The  $^{44}\text{Sc}$  lines were fitted with two Gaussians of equal intensity at fixed positions and with no line broadening.

The obtained best-fit parameters together with their 1  $\sigma$  confidence levels are given in Table 1. The best-fit model is found with a pure power-law continuum spectrum and a  $^{44}\text{Sc}$  line flux of  $(2.2 \pm 0.5) \times 10^{-5} \text{ cm}^{-2} \text{ s}^{-1}$  in each line ( $\chi^2 = 9.5$  for 10 degrees of freedom [dof]), consistent with previous COMPTEL and *BeppoSAX* PDS measurements. Taken together, the  $^{44}\text{Sc}$  lines are detected at the 4.5  $\sigma$  confidence level ( $\Delta\chi^2 = 20$ ), and each is individually detected at 3  $\sigma$  above the continuum emission. Relaxing the constraints on the line positions and width results

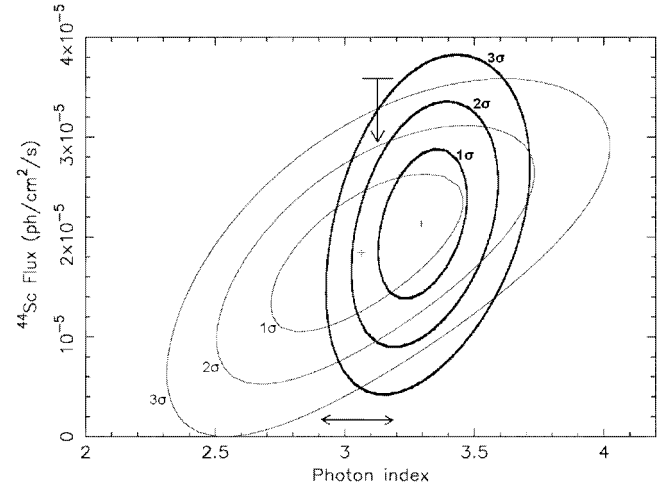


FIG. 4.—Confidence ellipses for the combination of the  $^{44}\text{Sc}$  line flux and the power-law photon index in the 21–120 keV band with IBIS/ISGRI (thick lines) and in the 30–100 keV band with *BeppoSAX* PDS (thin lines; Vink et al. 2001). The vertical arrow corresponds to the *Rossi X-Ray Timing Explorer* (RXTE) upper limit at 90% confidence level on the  $^{44}\text{Sc}$  line flux (Rothschild & Lingefelter 2003), and the horizontal arrow presents the first RXTE and OSSE measurements of the photon index (Allen et al. 1997).

in fitted line flux ( $2.3 \pm 0.5 \times 10^{-5} \text{ cm}^{-2} \text{ s}^{-1}$ ), positions ( $67.8 \pm 1.6$  and  $77.4 \pm 1.4$  keV), and width ( $< 1.6$  keV) consistent with the expected values and does not improve the fit ( $\chi^2 = 9.5$  for 7 dof). The 3  $\sigma$  upper limit on the line broadening translates to a nonconstraining upper limit of  $\sim 14,000 \text{ km s}^{-1}$  for the expansion velocity. For the `srcut` model, the flux density at 1 GHz and the radio spectral index were fixed to 2720 Jy and 0.77 (Green 2005). We find a  $\chi^2$  of 18.5 for 11 dof. According to the *F*-test, a power law is favored over the `srcut` model at 2.5  $\sigma$  (98.8%). It would be also the case of any other model that predicts a substantial steepening of the continuum emission above 50 keV. From Table 1, it is clear that the estimate of the  $^{44}\text{Sc}$  line flux is sensitive to this continuum modeling, and we then explored the correlation between the  $^{44}\text{Sc}$  line flux and the power-law photon index. Figure 4 presents such a correlation diagram. A detailed analysis of the nature of the hard X-ray continuum, its effect on the  $^{44}\text{Sc}$  line flux estimate, and the results obtained with the *INTEGRAL* SPI data will be presented in a forthcoming paper (J. Vink et al. 2006, in preparation).

#### 4. DISCUSSION

The IBIS/ISGRI observations confirm the presence of the two low-energy  $^{44}\text{Sc}$   $\gamma$ -ray lines in Cas A. By performing a weighted average of the three independent measurements of COMPTEL, *BeppoSAX* PDS (Vink et al. 2001), and ISGRI, we find a line flux of  $(2.5 \pm 0.3) \times 10^{-5} \text{ cm}^{-2} \text{ s}^{-1}$ . If we take into account uncertainties on its age (Thorstensen et al. 2001), distance (Reed et al. 1995), and  $^{44}\text{Ti}$  lifetime (Vink 2005), this is translated into an initial synthesized  $^{44}\text{Ti}$  mass of  $1.6_{-0.3}^{+0.6} \times 10^{-4} M_\odot$ . This mass of ejected  $^{44}\text{Ti}$  is generally thought to be

TABLE 1  
SPECTRAL MODEL FITS

Model	$^{44}\text{Sc}$ Flux ( $10^{-5} \text{ photons cm}^{-2} \text{ s}^{-1}$ )	Power-Law Index	Total Flux in the 21–120 keV Range ( $10^{-12} \text{ ergs cm}^{-2} \text{ s}^{-1}$ )	Flux Density at 1 GHz (Jy)	Radio Index	Roll-off Energy (keV)	$\chi^2/\nu$
Power law .....	$2.2 \pm 0.5$	$3.3 \pm 0.1$	$37.5 \pm 1.5$	...	...	...	9.5/10
<code>srcut</code> .....	$2.9 \pm 0.5$	...	...	2720 (fixed)	0.77 (fixed)	$0.97 \pm 0.02$	18.5/11

unusually large (or for few specific cases, marginally consistent) in comparison with spherical explosion models of WW95 and TNH96 (Timmes et al. 1996). Moreover, in the standard frame where  $^{44}\text{Ti}$  and  $^{56}\text{Ni}$  are coproduced during the first stages of the explosion, Cas A should have been a very bright,  $^{56}\text{Ni}$ -rich SN, in contrast with its nondetection or with Flamsteed's historical record. However, the large  $^{44}\text{Ti}/^{56}\text{Ni}$  ratio could be explained by the high degree of asymmetries (Nagataki et al. 1998). The high  $^{44}\text{Ti}$  yield thus supports the idea that Cas A is the result of an asymmetric and/or a relatively more energetic explosion, consistent with other observational evidence (Vink 2004; Hwang et al. 2004).

Anyway, the  $^{44}\text{Ti}$  production in core-collapse SNe is highly sensitive to the network used to compute nuclear reactions. With the recent revised  $^{40}\text{Ca}(\alpha, \gamma)^{44}\text{Ti}$  reaction rate (Nassar et al. 2006), theoretical models become more compatible with the  $^{44}\text{Ti}$  yield deduced from IBIS/ISGRI and previous observations. However, this would make the lack of other Galactic  $^{44}\text{Ti}$  sources an even more serious problem: several  $\gamma$ -ray line surveys (Dupraz et al. 1997; Renaud et al. 2004; The et al. 2006) have highlighted the problem of the “young, missing, and hidden” Galactic SNe, those that should have occurred since Cas A and are still not detected through the line emission from  $^{44}\text{Ti}$  decay. This would strengthen the idea that Cas A is peculiar (Young et al. 2006). On the other hand, the high  $^{44}\text{Ti}$  yield of both Cas A and SN 1987A (Fransson & Kozma 2002) is more in accordance with the solar  $^{44}\text{Ca}/^{56}\text{Fe}$  ratio, whereas this ratio is underpredicted by current spherically symmetric explosive nucleosynthesis models (Prantzos 2004; Young et al. 2006).

Besides the robustness provided by these IBIS/ISGRI spectroimaging observations, the main improvements compared to previous observations (Vink et al. 2001; Rothschild & Lingenfelter 2003) are the improved spectral resolution and the improved significance of the detection of the hard X-ray non-thermal continuum up to 100 keV well fitted by a single power law. The latter gives more stringent constraints on both the line intensities and the underlying continuum. Therefore, the scenario of a synchrotron radiation by TeV electrons (Allen et al. 1997) as modeled by Reynolds & Keohane (1999) seems not appropriate in the case of Cas A. On the other hand, the model developed by Laming (2001a, 2001b), implying a nonthermal bremsstrahlung emission of suprathermal electrons, could be an alternative scenario. Based on this firm detection of the  $^{44}\text{Sc}$  lines with IBIS/ISGRI, the expected results with SPI, thanks to its fine spectral resolution ( $\Delta E \sim 2$  keV FWHM at 1 MeV), should help us for the first time to constrain the kinematics of the innermost layers of the explosion (J. Vink et al. 2006, in preparation).

The present work is based on observations with *INTEGRAL*, an ESA project with instruments and science data center funded by ESA members states (especially the PI countries: Denmark, France, Germany, Italy, Switzerland, Spain, Czech Republic, and Poland, and with the participation of Russia and the US). ISGRI has been realized and maintained in flight by CEA-Saclay/DAPNIA with the support of CNES.

## REFERENCES

- Aharonian, F., et al. 2001, A&A, 370, 112  
 Ahmad, I., et al. 1998, Phys. Rev. Lett., 80, 2550  
 Allen, G. E., et al. 1997, ApJ, 487, L97  
 Ashworth, W. B., Jr. 1980, J. Hist. Astron., 11, 1  
 Chevalier, R. A., & Oishi, J. 2003, ApJ, 593, L23  
 den Hartog, P. R., Hermsen, W., Kuiper, L., Vink, J., in 't Zand, J. J. M., & Collmar, W. 2006, A&A, 451, 587  
 Diehl, R., & Timmes, F. X. 1998, PASP, 110, 637  
 Dupraz, C., et al. 1997, A&A, 324, 683  
 Fesen, R. A., & Becker, R. H. 1991, ApJ, 371, 621  
 Fransson, C., & Kozma, C. 2002, NewA Rev., 46, 487  
 Goldwurm, A., et al. 2003, A&A, 411, L223  
 Görres, J., et al. 1998, Phys. Rev. Lett., 80, 2554  
 Green, D. A. 2005, Mem. Soc. Astron. Italiana, 76, 534  
 Gros, A., et al. 2003, A&A, 411, L179  
 Hashimoto, T., et al. 2001, Nucl. Phys. A, 686, 591  
 Hwang, U., et al. 2004, ApJ, 615, L117  
 Iyudin, A. F., et al. 1994, A&A, 284, L1  
 Laming, J. M. 2001a, ApJ, 546, 1149  
 ———. 2001b, ApJ, 563, 828  
 Laming, J. M., & Hwang, U. 2003, ApJ, 597, 347  
 Lebrun, F., et al. 2003, A&A, 411, L141  
 Limongi, M., & Chieffi, A. 2003, ApJ, 592, 404  
 Nagataki, S., Hashimoto, M., Sato, K., Yamada, S., & Mochizuki, Y. 1998, ApJ, 492, L45  
 Nassar, H., et al. 2006, Phys. Rev. Lett., 96, 041102  
 Norman, E. B., et al. 1998, Phys. Rev. C, 57, 2010  
 Prantzos, N. 2004, in Fifth *INTEGRAL* Workshop on the *INTEGRAL* Universe, ed. V. Schönfelder, G. Lichten, & C. Winkler (ESA SP-552; Noordwijk: ESA), 15  
 Rauscher, T., et al. 2002, ApJ, 576, 323  
 Reed, J. E., Hester, J. J., Fabian, A. C., & Winkler, P. F. 1995, ApJ, 440, 706  
 Renaud, M., Lebrun, F., Ballet, J., Decourchelle, A., Terrier, R., & Prantzos, N. 2004, in Fifth *INTEGRAL* Workshop on the *INTEGRAL* Universe, ed. V. Schönfelder, G. Lichten, & C. Winkler (ESA SP-552; Noordwijk: ESA), 81  
 Renaud, M., Vink, J., Decourchelle, A., Lebrun, F., Terrier, R., & Ballet, J. 2006, NewA Rev., in press  
 Reynolds, S. P., & Keohane, J. W. 1999, ApJ, 525, 368  
 Rothschild, R. E., & Lingenfelter, R. E. 2003, ApJ, 582, 257  
 Stephenson, F. R., & Green, D. A. 2002, Historical Supernovae and Their Remnants (Oxford: Oxford Univ. Press)  
 The, L.-S., et al. 1996, A&AS, 120, 357  
 ———. 2006, A&A, 450, 1037  
 Thielemann, F. K., Nomoto, K., & Hashimoto, M. 1996, ApJ, 460, 408 (TNH96)  
 Thorstensen, J. R., Fesen, R. A., & van den Bergh, S. 2001, AJ, 122, 297  
 Timmes, F. X., Woosley, S. E., Hartmann, D. H., & Hoffman, R. D. 1996, ApJ, 464, 332  
 Ubertini, P., et al. 2003, A&A, 411, L131  
 Vink, J. 2004, NewA Rev., 48, 61  
 ———. 2005, Adv. Space Res., 35, 976  
 Vink, J., Kaastra, J. S., & Bleeker, J. A. M. 1996, A&A, 307, L41  
 Vink, J., & Laming, J. M. 2003, ApJ, 584, 758  
 Vink, J., Laming, J. M., Kaastra, J. S., Bleeker, J. A. M., Bloemen, H., & Oberlack, U. 2001, ApJ, 560, L79  
 Wietfeldt, F. E., Schima, F. J., Coursey, B. M., & Hoppe, D. D. 1999, Phys. Rev. C, 59, 528  
 Winkler, C., et al. 2003, A&A, 411, L1  
 Woosley, S. E., Langer, N., & Weaver, T. A. 1995, ApJ, 448, 315  
 Woosley, S. E., & Weaver, T. A. 1995, ApJS, 101, 181 (WW95)  
 Young, P. A., et al. 2006, ApJ, 640, 891